



Nuclear Regulatory Commission
 Exhibit # - AES000048-MA-BD01
 Docket # - 07007015
 Identified: 01/25/2011

Admitted: 01/25/2011
 Rejected:

Withdrawn:
 Stricken:

Exh. AES000048

Geological Society of America
 Special Paper 353
 2002

*Pliocene and Quaternary stratigraphic architecture
 and drainage systems of the Big Lost Trough,
 northeastern Snake River Plain, Idaho*

Jeffrey K. Geslin*
 Paul Karl Link
 James W. Riesterer

Department of Geosciences, Idaho State University, Pocatello, Idaho 83209, USA

Mel A. Kuntz

U.S. Geological Survey, Denver, Colorado 80225, USA

C. Mark Fanning

Research School of Earth Sciences, Australia National University, Canberra, ACT 2601, Australia

ABSTRACT

The geometry, volcanic-sedimentary stratigraphic architecture, and distribution of clastic sedimentary facies reflect a complex tectonic setting and fluctuations in climatic conditions during the past 2.5 m.y. in the Big Lost Trough on the eastern Snake River Plain. Interaction of the migrating Yellowstone hotspot and developing Basin and Range structures controlled the spatial distribution of volcanic rift zones that define the margins of the Big Lost Trough, an arid, underfilled basin. The volcanic-sedimentary stratigraphy of the basin is characterized by basaltic volcanic units that offlap eruptive centers and downlap into the basin, and clastic sedimentary units that onlap adjacent volcanic rift zones. Climatically influenced interactions of a fluvial-playa-eolian depositional system of the Big Lost River and a lacustrine system of Lake Terreton are reflected in the composition and architecture of the sedimentary basin fill.

Petrographic and U/Pb detrital-zircon geochronology analyses of subsurface sands compared with analyses of modern fluvial and eolian sands allow definitive determination of the provenance of the subsurface deposits. Petrographic and detrital-zircon data suggest that the Big Lost River has been the dominant source of sediment for at least the past 1 m.y. Big Lost River deposits found in the middle and northern parts of the basin suggest that the river system prograded northward during lowstands of Lake Terreton. Lowstands of Lake Terreton are also associated with development of an eolian system that reworked the fluvial deposits. The abundance of Big Lost River and eolian sands in the middle of the basin documents the effective damming of sediment by the volcanic rift zone that defines the northern basin margin. X-ray diffraction data suggest that subsurface playa or marginal lacustrine deposits along the northeastern basin margin contain abundant gypsum, indicating that ancient arid climate cycles were drier than the modern arid climate.

*Present address: ExxonMobil Upstream Research Company, P.O. Box 2189, Houston, TX 77252. E-mail: Jeff.K.Geslin@exxonmobil.com

Geslin, J.K., Link, P.K., Riesterer, J.W., Kuntz, M.A., and Fanning, C.M., 2002, Pliocene and Quaternary stratigraphic architecture and drainage systems of the Big Lost Trough, northeastern Snake River Plain, Idaho. *In* Link, P.K., and Mink, L.L., eds., *Geology, Hydrogeology, and Environmental Remediation: Idaho National Engineering and Environmental Laboratory, Eastern Snake River Plain, Idaho: Boulder, Colorado, Geological Society of America Special Paper 353*, p. 11-26.

INTRODUCTION

The Pliocene to Holocene Big Lost Trough is a small, closed sedimentary basin situated in the middle of the Idaho National Engineering and Environmental Laboratory (INEEL) on the eastern Snake River Plain, Idaho (Fig. 1). The northern INEEL, and the Test Area North (TAN) facility in particular, have been the focus of geological and hydrological investigations related to the remediation of contaminated groundwater in the Snake River Plain aquifer. Ultimately, it is crucial for hydrogeologic models and remediation technologies used in the northern INEEL to incorporate the stratal architecture of the vadose zone and aquifer in the northern end of the Big Lost Trough.

Volcanic rift zones and the Axial volcanic zone of the

Snake River Plain (Fig. 1) define the boundaries of the Big Lost Trough on all but its northwestern side, and the stratal architecture under the INEEL reflects the interaction between basaltic volcanism and sedimentary systems operating in the intervening basin. The Lost River Range, Lemhi Range, and Beaverhead Mountains, part of the Basin and Range system, are located along the northwestern basin margin. Streams in valleys between these ranges, including the Big Lost River, Little Lost River, and Birch Creek, are the dominant source of clastic sediments in the Big Lost Trough (e.g., Geslin et al., 1999). The Circular Butte-Kettle Butte volcanic rift zone defines a low-relief ridge on the northeastern end of the Big Lost Trough, and serves as a barrier between the basin and the adjacent Mud Lake subbasin (Fig. 1; e.g., Anderson and Bowers, 1985; Geslin et al., 1997; Mark and Thackray, this volume).

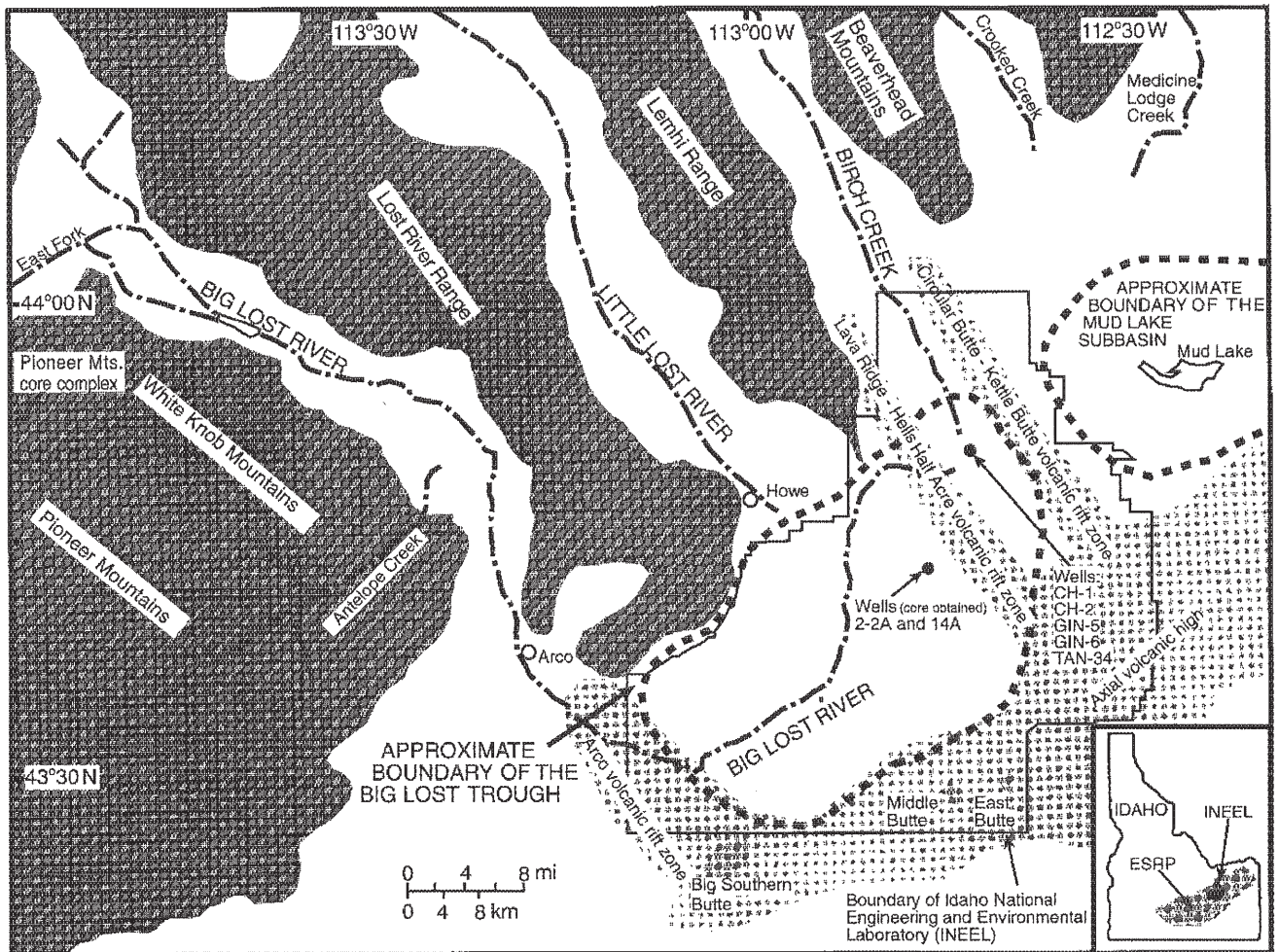


Figure 1. Map of study area showing location of approximate boundary of Big Lost Trough, adjacent basin and range features, streams that flow into basin, approximate locations of volcanic features on Snake River Plain, wells at Test Area North (CH-1, CH-2, GIN-5, GIN-6, TAN-34), and wells in middle of basin (2-2A, 14A).

The elevated topographic axis of the eastern Snake River Plain defines the southeastern side of the Big Lost Trough, and the Arco volcanic rift zone defines its southwestern border.

In this chapter we present the stratigraphic relationships of intercalated basalt flows and clastic sedimentary units in the northern Big Lost Trough, and discuss compositional analyses of sediments on the surface and in the shallow subsurface. We also document, using the results of detailed provenance analysis, the drainage history of the fluvial systems that deliver sand and gravel to the basin. These results predict that, in the upper part of Big Lost Trough strata, there is a progressively increasing abundance of high-permeability sediments (sands and gravels) from the northern end to the middle of the basin. X-ray diffraction analyses suggest that surficial fine-grained lacustrine

and playa sediments, as well as subsurface fine-grained sediments from the middle of the basin, are composed predominantly of smectite, kaolinite, and chlorite; this probably reflects weathering of volcanic and fine-grained sedimentary rocks in fluvial source areas. Fine-grained subsurface sediments found at the northeastern basin margin, in the vicinity of the TAN facilities, contain abundant gypsum, reflecting evaporative depositional conditions.

GEOLOGIC SETTING

The Big Lost Trough is located within the eastern Snake River Plain, a semiarid lava- and loess-mantled plain that cuts across the northwest-trending Basin and Range structure of

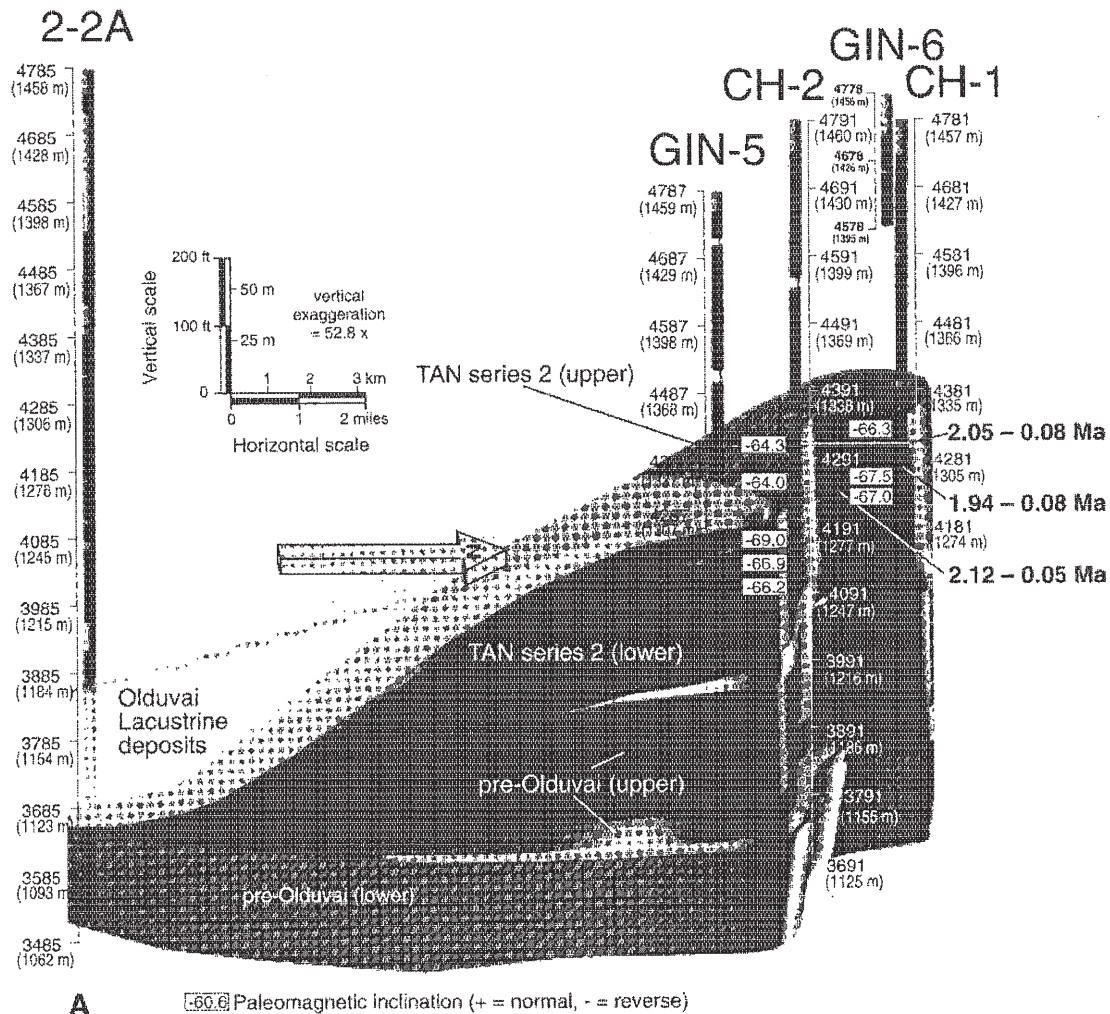


Figure 2. Three-dimensional correlation diagrams showing basalt flow groups and clastic sediments from northeastern basin margin (wells CH-1, CH-2, GIN-5, GIN-6) to middle of basin (well 2-2A). A: 2 Ma. B (page 14): 1 Ma. C (page 15): Modern. Well locations are shown in Figure 1. Basalt is darkly shaded and sedimentary units are lightly shaded. Abbreviations for lava flows Q-R and IJ reflect terminology of Hughes et al. (this volume).

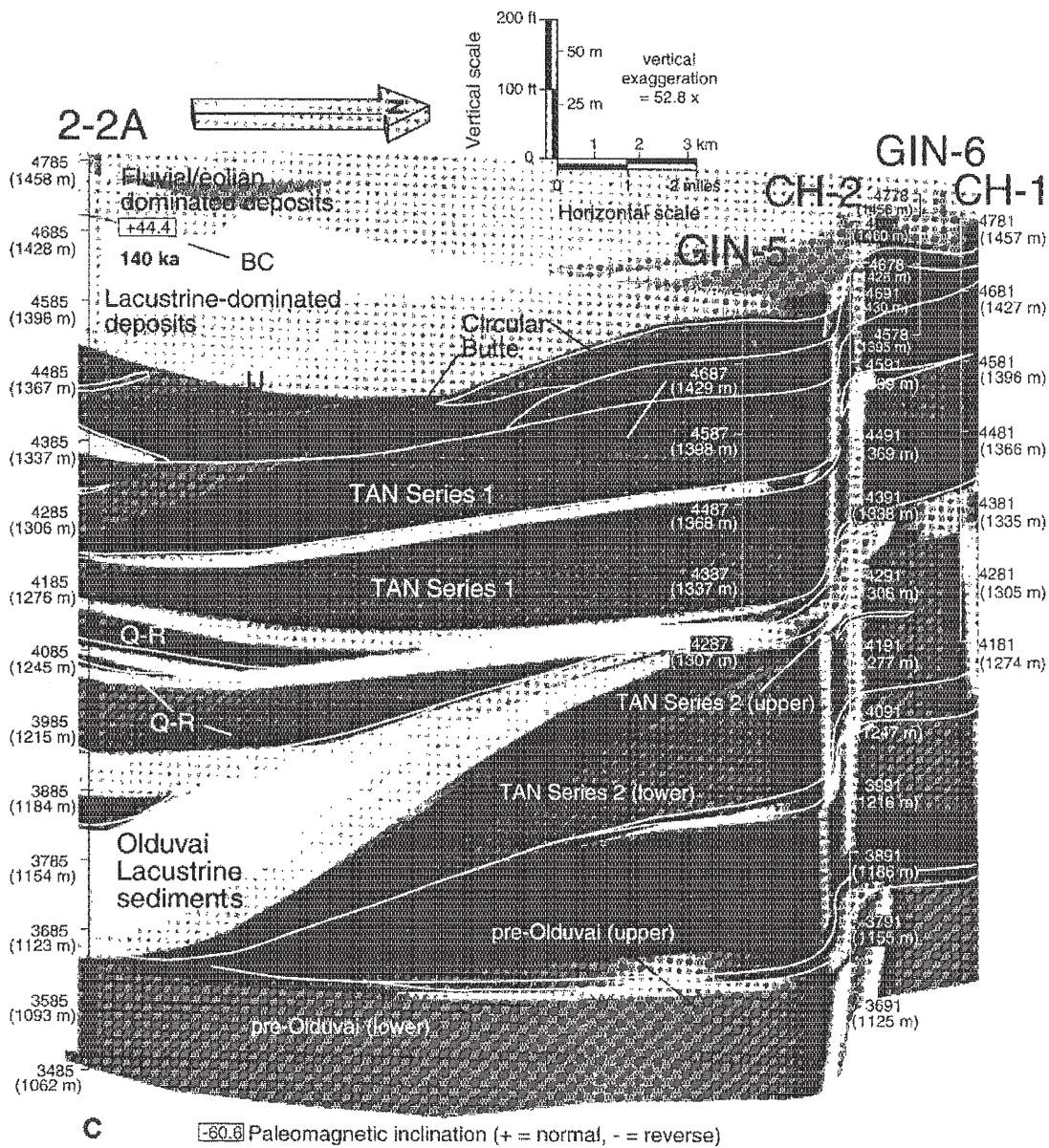


Figure 2. (continued)

also include small shield volcanoes and rhyolite domes (e.g., Kuntz et al., 1994). Basalt flows erupted along volcanic rift zones that parallel the northwest-southeast orientation of the adjacent Basin and Range structures (e.g., Kuntz et al., 1992). One of these volcanic rift zones, the Circular Butte–Kettle Butte volcanic rift zone, defines the northeastern end of the Big Lost Trough (Fig. 1). The stratigraphic architecture of the northern end of the basin (see following) reflects the interaction between basaltic volcanism along this volcanic rift zone and sedimentation in the basin.

Sediments are delivered to the Big Lost Trough primarily by three fluvial systems: the Big Lost River, the Little Lost River, and Birch Creek, which drain mountains to the northwest of the basin (Fig. 1; Geslin et al., 1999). Small streams that drain the southern end of the Beaverhead Mountains, north of the basin, and eolian systems operating on the eastern Snake River Plain contribute volumetrically less abundant clastic sediments. Eolian processes primarily winnow and redeposit sediments delivered by the fluvial systems. Examination of the modern configuration of the fluvial systems shows that both the

Little Lost River and Birch Creek have relatively small drainage areas and terminate in playas or sinks at the mouths of their respective valleys. However, the Big Lost River has a relatively large drainage area in the mountains of central Idaho and it traverses nearly the entire length of the Big Lost Trough, terminating in a series of playas near the northern end of the basin (Fig. 1; Kuntz et al., 1994).

The stratigraphic architecture of basalt flows and fluvial, eolian, playa, and lacustrine sediments in the Big Lost Trough controls groundwater flow, both in the vadose zone and the Snake River Plain aquifer (e.g., Mark and Thackray, this volume). In the Snake River Plain aquifer, ~60 m below the surface at the northern end of the Big Lost Trough, flow is to the south and southwest, driven by the regional head of the Mud Lake system (e.g., Whitehead; 1992; Spinazola, 1994). The regional flow in the aquifer suggests that as groundwater contaminants below the TAN facility migrate, their transport rate will be increasingly influenced by the hydrologic properties of sediments in the basin (see Mark and Thackray, this volume).

TECTONIC AND CLIMATIC SETTING

The Big Lost Trough is an arid, underfilled basin (cf. Carroll and Bohacs, 1999). It is underfilled because fluvial and lacustrine systems never breach basin margins defined by the surrounding topographically high volcanic rift zones. Generally, the basin geometry is a byproduct of these volcanic rift zones; however, fluvial systems that transport sediment into the basin are controlled by adjacent Basin and Range structures. The volcanic rift zones that define the northeastern and southwestern basin margins are generally collinear with Basin and Range structures adjacent to the Snake River Plain. Both the Basin and Range structures and volcanic rift zones are related to regional northeast to southwest extension (Kuntz et al.,

1992). Local subsidence of the Big Lost Trough could have resulted from crustal thinning and contraction related to the rhyolite caldera history of the Snake River Plain, specifically the 6.0 Ma Blue Creek caldera that underlies the area (Kuntz et al., 1992; Morgan, 1992; Blair and Link, 2000). Large-scale subsidence of the eastern Snake River Plain is probably due to both thermal contraction and loading by a midcrustal mafic sill (McQuarrie and Rodgers, 1998). Therefore, the tectonic development of the Big Lost Trough represents complex interactions between the migration of the Yellowstone hotspot and Basin and Range extension.

Sedimentation in the Big Lost Trough was dominated by eolian, fluvial, and playa systems during drier climatic conditions and a shallow lacustrine system, Lake Terreton, during wetter climatic conditions (Geslin et al., 1997, 1999; Gianniny et al., 1997; Blair and Link, 2000). Pleistocene Lake Terreton existed intermittently in both the Big Lost Trough and Mud Lake subbasin for the past ~2 m.y. (Stearns et al., 1939; Scott, 1982; Gianniny et al., this volume; Bestland et al., this volume). The low-relief nature of the surface of the eastern Snake River Plain probably resulted in very rapid fluctuations in the lateral extent of Lake Terreton; therefore, lacustrine sediments in the area provide a fairly sensitive indicator of relatively wet climates. Geslin et al. (1999) suggested that fluvial-playa-eolian systems operating today are analogous to depositional systems that operated in the Big Lost Trough during Pleistocene and Holocene dry climates.

VOLCANIC AND SEDIMENTARY STRATIGRAPHY

The stratigraphy of the Big Lost Trough is somewhat complex because basaltic volcanic units offlap eruptive centers and downlap into the basin, while clastic sedimentary units onlap adjacent volcanic rift zones (e.g., Hughes et al., 1998). Three-

TABLE 1. CATEGORIES USED FOR SAND POINT COUNTS OF FRAMEWORK GRAINS AND RECALCULATED PLOTS

Grain category definitions	Categories*	Recalculated parameters
Qp	Aphanitic polycrystalline quartz	Qp
Qm	Monocrystalline quartz	Qm
P	Plagioclase feldspar	P
K	Potassium feldspar	K
Lvv	Vitric volcanic lithic fragments	Lv
Lvf	Felsitic volcanic lithic fragments	Lv
Lvml	Microplitic volcanic lithic fragments	Lv
Lvl	Lathwork volcanic lithic fragments	Lv
Lmi	Low-grade metaigneous lithic fragments	Lmv
PolyM	Polycrystalline phyllosilicates	Lms
QMF(t)	Quartz-mica-feldspar aggregate with tectonite fabric	Lms
QMF(a)	Quartz-mica-feldspar aggregate without tectonite fabric	Lms
Ls(arg)	Argillaceous sedimentary lithic fragments	Ls
Ls(cb)	Carbonate sedimentary lithic fragments	Ls
Mica	Monocrystalline phyllosilicates	M
Dense	Dense mineral grains	D
C	Carbonate cement (not a grain category)	C
		QFLt: Q = Qm F = P + K Lt = Lv + Lm + Ls + Qp
		LmLvLst: Lm = Lm Lv = Lv Lst = Ls + Qp
		QpLvmlsm: Qp = Qp Lvm = Lv + Lmv Lsm = Ls + Lms
		QmKP: Qm = Qm K = K P = P

*See Ingersoll et al. (1984)

dimensional stratigraphic diagrams, constructed from well data, were created to illustrate the development of the stratal architecture in the northern end of the Big Lost Trough (Fig. 2). Figure 2 encompasses a region that includes TAN, the focus of geologic, hydrologic, and environmental studies, and areas hydrologically downgradient to the south. The three-dimensional stratigraphic diagrams correlate basalt flow groups (flow group classification based on Hughes et al. [this volume] as modified from Lanphere et al. [1994] and Anderson and Bowers [1995]) and clastic sedimentary successions from wells CH-1, CH-2, GIN-5, GIN-6, and TAN-34 at TAN to well 2-2A near the middle of the basin (Fig. 1). Geochronology data for basalt flow groups are from whole-rock $^{40}\text{Ar}/^{39}\text{Ar}$ analyses (Lanphere et al., 1994). A single date of 140 ka in the upper sedimentary succession in well 2-2A is from Geslin et al. (1999) and is based on amino acid racemization in ostracode shells. Paleomagnetic data are from Champion et al. (1988). The stratigraphy shown

in these diagrams represents basaltic lava flows and clastic sediments deposited over the past ~2.5 m.y.

The stratal architecture of the northern end of the basin (Fig. 2) documents the construction of basaltic eruptive centers along the Circular Butte-Kettle Butte volcanic rift zone. The southward downlapping or offlapping of pre-Olduvai, TAN series 1 and 2, and Circular Butte basalt flow groups (Fig. 2), along with surface data (Kuntz et al., 1994), suggests that many of the flows moved generally northeast to southwest, from the volcanic rift zone toward the middle of the basin. Basalt flow group geometry, along with the northward onlap of sediments onto the volcanic rift zone, suggests that the volcanic rift zone was a positive topographic feature throughout basin history. Some of the smaller post-Olduvai flow groups present in well 2-2A (Fig. 2B) are not present in wells along the northern basin margin, and could have erupted from a volcanic center to the south, and then flowed northward into the basin. The strati-

TABLE 2. RECALCULATED MODAL POINT-COUNT DATA FOR SURFICIAL SEDIMENTS OF THE BIG LOST TROUGH AND ADJACENT DRAINAGES

Sample No.	QmFLt			LmLvLst			QpLvLsm			QmKP		
	Qm	F	Lt	Lm	Lv	Lst	Qp	Lvm	Lsm	Qm	K	P
Big Lost River channel												
1PL96	20.4	14.9	64.7	12.3	69.4	18.3	7.9	69.4	22.7	57.8	0.0	42.2
7JG97	22.4	25.1	52.5	35.3	41.8	22.9	10.4	41.8	47.8	47.1	19.6	33.3
8JG97	12.9	15.8	71.4	32.3	45.3	22.4	13.7	45.3	41.0	44.9	16.7	38.4
9JG96	18.3	14.6	67.1	1.2	67.9	31.0	11.2	67.9	20.9	55.6	17.3	27.2
10JG96	12.5	15.7	71.8	18.0	67.1	15.0	8.7	67.1	24.3	44.3	21.4	34.4
15JG96	27.3	10.6	62.1	9.1	67.1	23.8	5.2	67.1	27.8	72.1	4.5	23.4
mean	19	16	65	18	60	22	10	60	31	54	13	33
σ	6	5	7	13	13	5	3	13	11	11	9	7
Little Lost River channel												
3JG97	36.0	10.5	53.4	29.4	44.0	26.6	13.8	44.0	42.2	77.4	7.9	14.7
4JG97	10.7	2.8	86.5	4.0	5.3	90.7	25.7	5.3	69.0	79.0	6.5	14.5
5JG96	27.6	2.2	70.2	11.5	26.2	62.3	2.6	26.2	71.2	92.6	1.2	6.2
5JG97	37.0	7.4	55.6	18.9	47.2	33.9	15.9	47.2	36.9	83.3	3.8	12.9
6JG97	40.9	4.9	54.2	18.7	45.9	35.4	25.7	45.9	28.4	89.4	0.5	10.1
mean	31	6	64	17	34	50	17	34	49	84	4	12
σ	12	4	14	9	18	27	10	18	19	7	3	4
Birch Creek channel												
1JG97	18.0	6.4	75.6	6.2	3.8	90.0	35.0	3.8	61.2	73.9	21.8	4.2
2JG97	14.6	5.8	79.6	54.7	3.9	41.4	20.7	3.9	75.4	71.4	19.4	9.2
3JG96	15.6	4.1	80.2	0.0	40.3	59.7	10.0	40.3	49.7	79.2	7.3	13.5
11JG96	14.9	9.2	75.8	6.9	13.0	80.1	12.5	13.0	74.5	61.7	20.0	18.3
mean	16	6	78	17	15	68	20	15	65	72	17	11
σ	1	2	2	26	17	22	11	17	12	7	7	6
Small drainages north of Big Lost Trough (Medicine Lodge Creek)												
1JR97	32.6	4.9	62.5	20.8	28.3	50.8	26.1	28.3	45.6	87.0	4.3	8.7
2JR97	65.9	6.3	27.8	29.5	19.1	51.4	31.4	19.0	49.5	91.2	6.6	2.2
4JR97	57.4	6.9	35.7	39.2	16.9	43.8	33.1	16.9	50.0	89.3	6.0	4.7
5JR97	32.4	9.3	58.3	38.5	22.5	39.0	22.5	22.5	55.0	77.6	6.3	16.1
mean	47	7	46	32	22	46	28	22	50	86	6	8
σ	17	2	17	8	5	6	5	5	4	6	1	6
Eolian (sand dunes)												
1JG96	22.8	29.6	47.6	9.2	52.1	38.7	2.8	52.1	45.2	43.5	17.6	38.9
2PL96	28.0	5.4	66.6	1.2	17.6	81.1	13.9	17.6	68.4	84.0	0.0	16.0
7JR96	31.5	16.0	52.6	5.4	43.8	50.8	8.7	43.8	47.5	66.5	5.0	28.4
12JG96	27.8	15.1	57.1	15.6	49.4	34.9	2.2	49.4	48.3	69.4	8.9	26.2
14JG96	30.0	9.8	60.2	8.2	30.9	61.0	1.1	30.9	68.0	75.3	7.9	16.9
mean	28	15	57	8	39	53	6	39	55	67	8	25
σ	3	9	7	6	14	19	6	14	12	15	7	9

graphically highest basalt flow group at the northern end of the Big Lost Trough (Circular Butte flows, Fig. 2C) is ca. 1 Ma, suggesting that the area has been volcanically quiet through much of the Pleistocene (Anderson and Lewis, 1989; Anderson, 1991; Anderson et al., 1996).

A thick sedimentary succession is present, most notably in the upper part of the stratigraphic section near the site of well 2-2A, in the north-central part of the basin (Fig. 2C; Anderson and Bowers, 1995; Geslin et al., 1997; 1999; Blair and Link, 2000). Although there are no data on interwell geometry, these sediments apparently onlap the northern basin margin (Fig. 2C), documenting the closed nature of the basin. Strata in the upper part of well 2-2A record the interaction of eolian, fluvial, playa, and lacustrine depositional systems (e.g., Geslin et al., 1997, 1999; Gianniny et al., 1997). These strata document a general shift from lacustrine-dominated sedimentation to fluvial- and/or eolian-dominated sedimentation, suggesting an overall drying of the climate (e.g., Bestland et al., this volume). In this volume Geslin et al. and Gianniny et al. argue that modern fluvial, playa, and eolian systems are excellent analogs for ancient depositional systems operating in the basin during relatively dry climatic conditions; lacustrine clays and fine sands deposited in Lake Terreton probably represent relatively wetter climatic conditions. Gianniny et al. (this volume) discuss the timing of multiple recent fluctuations of Lake Terreton. Bestland et al. (this volume) discuss older lacustrine sedimentation documented in the deeper core from well 2-2A (Fig. 2A) and emphasize weak paleosols developed on fluvial, playa, eolian, and lacustrine sediments in the upper part of the 2-2A core.

COMPOSITIONAL ANALYSIS OF SEDIMENTARY UNITS

We examined both modern and shallow subsurface sands from the Big Lost Trough using petrographic analysis. Provenance interpretations of fluvial sands, based on modal recalculation of petrographic data, were supported by U/Pb geochronology of detrital zircons. Provenance results, particularly at the northern end of the basin, are used to interpret the evolution of the fluvial systems and document the role of volcanic eruptive centers in controlling the distribution of depositional systems.

The compositions of modern and shallow subsurface fine-grained sediments were evaluated using semiquantitative X-ray diffraction analysis, and are used to characterize depositional environments. Hughes et al. (this volume) present compositional analyses of the basalts and correlations of the basalt flow groups found in the Big Lost Trough.

Provenance of sands

Petrographic analyses. Sand samples were collected from modern fluvial and eolian deposits, and from core retrieved from wells in the middle and northern parts of the basin (Fig. 1). All

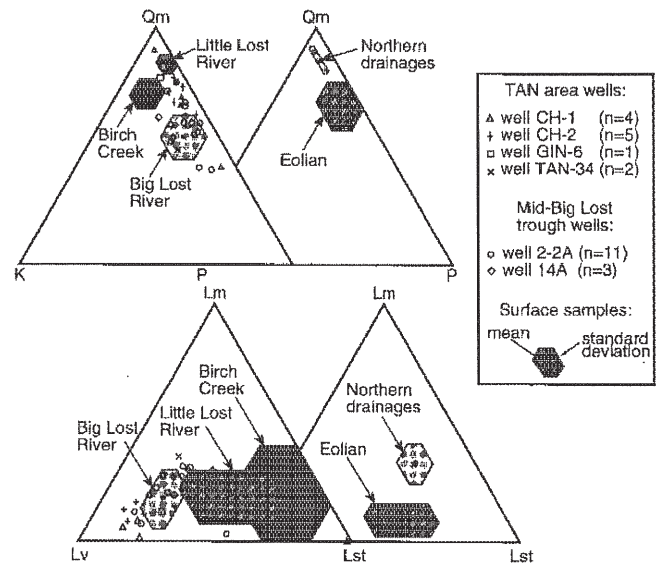


Figure 3. Standard ternary plots of detrital modes from petrographic analysis of sand samples. Qm—monocrystalline quartz, K—potassium feldspar, P—plagioclase feldspar, Lm—metamorphic lithic grains, Lv—volcanic lithic grains, Lst—total sedimentary lithic grains. Polygons represent mean and standard deviation for samples collected from modern drainages (Big Lost River, $n = 6$; Little Lost River, $n = 5$; Birch Creek, $n = 4$; northern drainages, $n = 4$; eolian deposits, $n = 5$). Symbols represent individual samples collected from wells (locations in Fig. 1) in central and northern parts of Big Lost Trough ($n = 29$).

modern fluvial systems that flow into the Big Lost Trough, including the Big Lost River, Little Lost River, and Birch Creek, were sampled, as were several small streams that flow out of the southern Beaverhead Mountains and terminate near the northeastern margin of the basin. Sand samples were examined petrographically; compositions were determined by the Gazzi-Dickinson point-count method (Ingersoll et al., 1984); raw point-count data were recalculated into detrital modes (Table 1). Samples from modern fluvial and eolian deposits, summarized in Table 2, were first compared to each other by plotting detrital mode data on ternary diagrams (Fig. 3). The source areas of the modern streams are generally well differentiated using fields defined by the statistical average and standard deviation for the samples (Fig. 3). Big Lost River sands are distinguished by abundant volcanic lithic material, probably reflecting both the abundance of Challis volcanic rocks in the source area and the abundant Snake River Plain basalts over which the stream flows in its lower reach. Modern eolian sands have an average composition that overlaps several of the fluvial fields (Fig. 3), indicating mixing and redeposition.

To evaluate the provenance of shallow subsurface sands, their recalculated modal compositions (Table 3) were compared to modern sands by plotting subsurface samples individually on the ternary diagrams (Fig. 3). The majority of the shallow subsurface sand samples have modal compositions that are similar

TABLE 3. RECALCULATED MODAL POINT-COUNT DATA FOR SUBSURFACE SEDIMENTS OF THE BIG LOST TROUGH

Sample No.	Depth (m)	QmFLt			LmLvLst			QpLvLsm			QmKP		
		Qm	F	Lt	Lm	Lv	Lst	Qp	Lvm	Lsm	Qm	K	P
Corehole 2-2A													
18JG96	19.8	26.7	17.4	55.9	21.0	58.0	21.0	17.8	58.0	24.2	60.5	9.7	29.8
19JG96	21.3	24.4	14.8	60.8	21.8	48.2	29.9	25.4	48.2	26.4	62.3	8.2	29.5
20JG96	36.6	26.7	17.9	55.3	31.9	44.1	23.9	16.0	44.1	39.9	59.9	4.1	36.0
21JG96	41.2	20.9	30.4	48.9	4.4	44.4	51.2	0.0	44.4	55.6	40.7	13.9	45.4
22JG96	42.4	30.9	20.9	48.2	22.8	60.8	16.4	4.2	60.8	34.9	59.6	7.4	33.0
23JG96	44.8	15.1	22.1	62.8	13.1	73.5	13.5	2.9	73.5	23.6	40.5	9.8	49.7
24JG96	50.6	23.4	11.5	65.1	23.9	39.1	37.0	25.0	39.1	35.9	67.1	5.9	27.0
25JG96	55.2	15.7	13.0	71.3	27.9	49.1	22.9	15.6	49.1	35.3	54.7	9.5	35.8
26JG96	58.6	27.2	12.7	60.2	28.1	56.1	15.8	10.1	56.1	33.8	68.2	5.3	26.5
27JG96	72.4	30.2	9.3	60.5	20.4	64.6	15.0	10.2	64.6	25.2	76.5	4.5	19.0
28JG96	75.3	25.5	17.4	57.1	29.3	55.0	15.7	12.4	55.0	32.5	59.4	8.6	32.1
29JG96	113.6	19.4	18.0	62.7	19.9	56.0	24.1	17.3	56.0	26.7	51.9	19.1	29.0
30JG96	118.8	21.6	17.2	61.2	32.2	46.4	21.4	11.2	46.4	42.4	55.6	7.0	37.4
31JG96	191.9	41.2	15.2	43.8	7.7	74.0	18.4	16.3	74.0	9.7	73.0	10.3	16.7
Corehole TAN CH1													
34JG96	122.5	44.7	4.7	50.6	0.0	1.6	98.4	25.4	1.6	73.0	90.5	5.4	4.1
36JG97	125.4	17.4	25.2	57.4	1.9	77.4	20.6	7.1	77.4	15.5	40.9	6.1	53.0
37JG96	136.0	33.4	16.2	50.3	6.0	81.2	12.8	7.4	81.2	11.4	67.3	6.8	25.9
38JG96	136.2	31.1	12.7	56.1	8.8	74.5	16.8	11.7	74.5	13.9	71.0	4.7	24.3
Corehole TAN CH2													
39JG96	73.0	35.4	12.9	51.7	12.5	70.1	17.4	15.8	70.1	14.1	73.3	7.2	18.0
41JG96	143.1	34.2	9.0	56.8	14.2	76.5	9.3	9.3	76.5	14.2	79.1	4.3	16.6
42JG96	224.2	35.8	16.2	47.5	9.3	77.6	13.1	9.8	77.6	12.6	68.3	9.4	22.3
43JG96	224.8	29.1	17.4	53.5	14.6	58.7	26.7	14.1	58.7	27.2	62.6	4.5	33.0
44JG96	225.5	32.2	10.6	57.1	17.2	70.6	12.3	10.8	70.6	18.6	75.2	3.3	21.6
Corehole GIN 6													
33JG96	35.7	32.8	8.7	58.5	13.2	64.0	22.8	12.7	64.0	23.2	79.0	9.3	11.7
Borehole 14A													
9JG97	4.2	26.0	18.0	56.0	29.9	35.6	34.4	7.3	35.6	57.1	59.0	15.1	25.9
10JG97	8.8	28.8	18.0	53.2	29.9	45.0	25.1	6.4	45.0	48.6	61.5	18.1	20.4
11JG97	15.0	17.4	15.3	67.2	27.2	51.9	20.9	13.9	51.9	34.2	53.2	16.9	29.9
Borehole TAN 34 (cuttings)													
15-20	4.6-6.1	36.7	11.2	52.1	19.0	48.6	32.4	22.4	48.6	29.0	76.7	4.1	19.2
25-30	7.6-9.1	19.5	21.2	59.3	35.7	46.2	18.1	11.6	46.2	42.2	47.9	18.4	33.7

to those of modern sands from the Big Lost River; a few samples are compositionally similar to modern eolian sands. These data suggest that the Big Lost River has been the dominant source of fluvial sands in the basin since at least the Pliocene.

The abundance of Big Lost River and eolian sands in the middle of the basin documents the effective damming of sediment by the volcanic rift zone that defines the northern basin margin (Fig. 2). These results also suggest that deposition by the Big Lost River in the middle of the basin is commonly associated with dry climatic conditions favorable for the development of an eolian system, similar to present-day conditions.

Detrital-zircon U/Pb geochronology. Sand samples for detrital-zircon analysis were collected from modern fluvial deposits, from shallow core retrieved from well 2-2A in the southern Big Lost Trough, and wells TAN-34, CH-1, and CH-2 at TAN. Detrital zircons were separated from the samples and ~50 zircon grains from each sample were analyzed on SHRIMP I at the Australian National University (Table 4). The ages of individual zircon grains were derived from the weighted mean of $^{206}\text{Pb}/^{238}\text{U}$ -, $^{207}\text{Pb}/^{235}\text{U}$ - and $^{207}\text{Pb}/^{206}\text{Pb}$ -corrected ages, and relative-probability spectra were created by assigning

Gaussian distributions to individual ages and errors and then summing them together in 1 m.y. bins.

It is easy to differentiate the detrital-zircon age spectra for the fluvial systems that provide sediment to the Big Lost Trough (Fig. 4). There are distinctive populations of detrital zircons in the sands from Birch Creek and the small northern drainages (Fig. 4, C-F): (1) several groups of <20 Ma zircons derived from Snake River Plain volcanic rocks; (2) 700-100 Ma zircons derived from the Cretaceous Idaho batholith (Worl et al., 1995); (3) ca. 500 Ma zircons derived from the Ordovician Beaverhead pluton exposed in the Beaverhead Mountains (Evans and Zartman, 1988); and (4) a large group of 1000-2000 Ma zircons and a small group of 2500-3000 Ma zircons likely recycled from Mesoproterozoic to Ordovician strata exposed in the Beaverhead Mountains and Lemhi Range (Oaks et al., 1977; Skipp and Link, 1992; Winston and Link, 1993). Detrital zircons from the Little Lost River (Fig. 4B) also contain a large Paleoproterozoic zircon population (1500-2000 Ma), but this sample can be differentiated from other samples by the presence of a large ca. 50 Ma zircon population, derived from the Eocene Challis Volcanic Group, and by the lack of 500 Ma and <20 Ma zircon populations. The detrital-zircon population in the Big Lost

TABLE 4. DETRITAL-ZIRCON AGE DATA FOR SURFACE AND SUBSURFACE SANDS OF THE BIG LOST TROUGH AND ADJACENT DRAINAGES

Sample 9JG96 Big Lost River			Sample 5JG96 Little Lost River			Sample 11JG96 Birch Creek			Sample 1JR96 Beaver Creek			Sample 2JR96 Crooked Creek			Sample 2JR97 Medicine Lodge Creek			Sample 50JG96 Well 2-2A 55.4 m					
Grain spot	Age $^{206}\text{Pb}/^{238}\text{U}$	\pm	Grain spot	Age $^{206}\text{Pb}/^{238}\text{U}$	\pm	Grain spot	Age $^{206}\text{Pb}/^{238}\text{U}$	\pm	Grain spot	Age $^{206}\text{Pb}/^{238}\text{U}$	\pm	Grain spot	Age $^{206}\text{Pb}/^{238}\text{U}$	\pm	Grain spot	Age $^{206}\text{Pb}/^{238}\text{U}$	\pm	Grain spot	Age $^{206}\text{Pb}/^{238}\text{U}$	\pm			
1.1	2628	57	1.1	1841	43	1.1	503	22	1.1	1851	40	1.1	1646	34	1.1	1669	47	1.1	1669	47	1.1	46.8	0.7
2.1	46.9	0.9	2.1	1614	70	2.1	498	32	2.1	50.2	1.2	3.1	2.1	0.1	2.1	2669	111	2.1	2669	111	2.1	2644	29
3.1	45.4	1.5	3.1	1774.4	36.1	3.1	1055	27	3.1	51.0	1.2	4.1	10.7	1.0	3.1	1730	44	3.1	1730	44	3.1	56.1	1.3
4.1	707	21	4.1	49.9	1.4	4.1	1859	44	4.1	52.1	1.2	5.1	7.7	0.7	4.1	1650	51	4.1	1650	51	4.1	47.0	1.3
5.1	611	40	5.1	1728	38	5.1	33.0	0.9	5.1	52.9	1.3	6.1	1817	50	5.1	1103	59	5.1	1103	59	5.1	46.8	1.0
6.1	46.6	1.8	6.1	49	2	6.1	1289	22	6.1	47.1	2.3	7.1	1399	32	6.1	1429	43	6.1	1429	43	6.1	971	22
7.1	46.5	1.5	7.1	1275.7	47.4	7.1	482	29	7.1	51.2	1.2	8.1	1775	34	7.1	1488	58	7.1	1488	58	7.1	1266	115
8.1	1441	59	8.1	2254	65	8.1	1.1	0.3	8.1	50.9	2.1	9.1	1048	44	8.1	1345	49	8.1	1345	49	8.1	1760	33
9.1	46.4	1.4	9.1	1666	35	9.1	1810	29	9.1	75.3	3.1	10.1	48.9	2.1	9.1	1627	32	9.1	1627	32	9.1	48.6	1.6
10.1	47.3	1.1	10.1	1728	35	10.1	496	13	10.1	91.9	2.0	11.1	1028	18	10.1	1835	46	10.1	1835	46	10.1	1760	50
11.1	49.6	1.5	11.1	1787	41	11.1	44.3	1.2	11.1	50.3	1.4	12.1	1548	64	11.1	1352	32	11.1	1352	32	11.1	48.6	1.0
12.1	48.6	2.0	12.1	1687.4	27.0	12.1	2574	148	12.1	50.9	1.3	13.1	6.5	0.4	12.1	1656	27	12.1	1656	27	12.1	51.5	1.3
13.1	52.9	2.4	13.1	2728	72	13.1	491	29	13.1	64.8	3.9	14.1	32.4	1.5	13.1	6.4	0.6	13.1	6.4	0.6	13.1	1767	23
14.1	50.9	4.7	14.1	51	2	14.1	485	13	14.1	49.2	1.1	15.1	11.9	0.7	14.1	536	26	14.1	536	26	14.1	1118	32
15.1	45.7	2.1	15.1	668	13	15.1	1665	36	15.1	2.7	0.3	16.1	26.9	7.6	15.1	1703	38	15.1	1703	38	15.1	88.0	2.8
16.1	49.9	2.0	16.1	50.6	1.8	16.1	46.8	1.6	16.1	1791	41	17.1	1598	44	16.1	1693	59	16.1	1693	59	16.1	83.3	2.2
17.1	49.1	1.5	17.1	1667	44	17.1	33.1	2.2	17.1	227	10	18.1	8.4	0.5	17.1	91.5	4.2	17.1	91.5	4.2	17.1	1922	50
18.1	48.3	2.3	18.1	1830	38	18.1	1408	25	18.1	50.4	1.7	19.1	1406	49	18.1	93.9	3.6	18.1	93.9	3.6	18.1	49.5	1.6
19.1	47.4	1.1	19.1	1744	50	19.1	1808	38	19.1	16.6	0.5	20.1	1610	29	19.1	1530	43	19.1	1530	43	19.1	49.2	1.2
20.1	52.4	2.2	20.1	1716.2	46.1	20.1	485	24	20.1	50.4	1.4	21.1	1738	37	20.1	18.4	9.5	20.1	18.4	9.5	20.1	11.3	1.3
21.1	689	39	21.1	1713.0	41.0	21.1	38.2	1.5	21.1	1083	22	22.1	1829	55	21.1	6.3	0.5	21.1	6.3	0.5	21.1	1690	28
22.1	47.9	1.3	22.1	1633	38	22.1	495	13	22.1	1406	52	23.1	1571	95	22.1	1588	105	22.1	1588	105	22.1	50.1	1.7
23.1	51.2	1.9	23.1	1707	44	23.1	1698	39	23.1	47.4	2.4	24.1	2079	38	23.1	92	2	23.1	92	2	23.1	46.0	1.3
24.1	42.8	1.0	24.1	1812	36	24.1	1809	46	24.1	49.9	1.5	25.1	1594	35	24.1	1072	25	24.1	1072	25	24.1	10.4	0.4
25.1	49.6	1.7	25.1	48	1	25.1	1570	45	25.1	1420	59	26.1	484	22	25.1	1750	72	25.1	1750	72	25.1	2047	44
26.1	49.0	1.2	26.1	1713.8	69.8	26.1	488	13	26.1	49.5	1.2	27.1	484	18	26.1	1750	37	26.1	1750	37	26.1	50.5	1.1
27.1	46.0	0.9	27.1	1402	74	27.1	462	13	27.1	7.6	1.4	28.1	1594	36	27.1	63.5	4.1	27.1	63.5	4.1	27.1	1768	39
28.1	674	16	28.1	48	3	28.1	1857	33	28.1	13.5	0.9	29.1	2682	60	28.1	1765	46	28.1	1765	46	28.1	46.8	1.3
29.1	1449	24	29.1	2546	49	29.1	1454	35	29.1	509	10	30.1	10.3	0.3	29.1	419	12	29.1	419	12	29.1	93.6	2.1
30.1	49.6	2.3	30.1	1815	51	30.1	1066	25	30.1	1729	40	31.1	1678	36	30.1	1205	44	30.1	1205	44	30.1	2262	32
31.1	570	15	31.1	1661	40	31.1	1418	29	31.1	2785	55	32.1	1777	40	31.1	1782	49	31.1	1782	49	31.1	1058	13
32.1	54.1	1.0	32.1	2615	62	32.1	266	7	32.1	48.8	2.7	33.1	2633	60	32.1	9.8	1.8	32.1	9.8	1.8	32.1	50.2	1.2
33.1	45.4	1.0	33.1	48	1	33.1	1661	38	33.1	48.0	1.7	34.1	47.9	1.1	33.1	101	2	33.1	101	2	33.1	46.5	1.4
34.1	48.0	1.2	34.1	501	13	34.1	498	28	34.1	1419	38	35.1	49.7	1.9	34.1	1770	27	34.1	1770	27	34.1	1658	23
35.1	48.1	1.5	35.1	2813	76	35.1	452	34	35.1	8.2	5.0	36.1	67.7	1.9	35.1	1774	82	35.1	1774	82	35.1	47.5	1.1
36.1	1248	32	36.1	1840	56	36.1	1081	25	36.1	11.0	7.3	37.1	1686	32	36.1	1715	52	36.1	1715	52	36.1	48.9	1.0
37.1	46.2	1.2	37.1	1355	51	37.1	1255	39	37.1	1275	43	38.1	1160	31	37.1	1789	40	37.1	1789	40	37.1	2180	64
38.1	43.8	2.2	38.1	49.5	1.7	38.1	463	16	38.1	1288	46	40.1	474	18	38.1	1730	39	38.1	1730	39	38.1	49.4	1.1
39.1	1245	32	39.1	1721	39	39.1	489	12	39.1	1288	46	40.1	6.7	0.8	40.1	1453	27	40.1	1453	27	40.1	47.2	0.8
40.1	53.8	2.9	40.1	1732	31	40.1	17.2	1.6	40.1	52.3	4.5	41.1	6.7	0.8	40.1	1007	21	40.1	1007	21	40.1	438	10
41.1	44.0	1.1	41.1	2025.0	45.7	41.1	46.2	1.9	41.1	97.3	3.6	42.1	3.5	0.8	41.1	1144	16	41.1	1144	16	41.1	45.5	1.1
42.1	49.5	2.0	42.1	1817	56	42.1	8.9	1.0	42.1	101	7	43.1	7.7	1.2	42.1	1007	21	42.1	1007	21	42.1	438	10
15.2	44.1	1.5	43.1	2694	45	43.1	1451	28	43.1	96.3	4.5	44.1	1743	38	43.1	1710	42	43.1	1710	42	43.1	45.3	0.9
19.2	46.3	2.0	44.1	1839	37	44.1	637	23	44.1	153	3	45.1	83	29	44.1	1010	51	44.1	1010	51	44.1	48.9	1.5
43.1	47.8	1.1	45.1	1959	77	45.1	6.4	0.8	45.1	97.6	1.4	46.1	929	30	45.1	1729	44	45.1	1729	44	45.1	48.4	1.0
44.1	44.6	1.7	46.1	1	0	46.1	6.6	1.4	46.1	77.3	5.7	48.1	1054	21	46.1	98.3	1.3	46.1	98.3	1.3	46.1	11.0	0.5
28.2	706	21	47.1	1761.8	28.6	47.1	106	6	47.1	77.3	5.7	48.1	13.9	0.5	47.1	1016	26	47.1	1016	26	47.1	613	27
20.2	49.9	1.8	48.1	2677.8	56.2	48.1	1431	54	48.1	48.5	1.2	49.1	1549	50	48.1	1694	34	48.1	1694	34	48.1	1979	55
12.2	50.8	2.1	49.1	1753	29	49.1	1787	37	49.1	1372	26	50.1	1708	35	49.1	395	7	49.1	395	7	49.1	47.9	1.2
13.2	50.2	1.6	50.1	1521	46	50.1	962	27	50.1	517	18				50.1	1069	65	50.1	1069	65	50.1	46.8	1.0

TABLE 4. DETRITAL-ZIRCON AGE DATA (continued)

Sample 51JG96 Well 2-2A 113.7 m				Sample 52JG96 Well 2-2A 191.9 m				Sample 3UG96 Well TAN 34 ~5.8 m				Sample 47JR96 Well CH 2 136.8 m				Sample 48JR96 Well CH 2 224.4 m				Sample 49JR96 Well CH 1 136.0 m			
Grain spot	Age $^{206}\text{Pb}/^{238}\text{U}$	\pm	Grain spot	Age $^{206}\text{Pb}/^{238}\text{U}$	\pm	Grain spot	Age $^{206}\text{Pb}/^{238}\text{U}$	\pm	Grain spot	Age $^{206}\text{Pb}/^{238}\text{U}$	\pm	Grain spot	Age $^{206}\text{Pb}/^{238}\text{U}$	\pm	Grain spot	Age $^{206}\text{Pb}/^{238}\text{U}$	\pm	Grain spot	Age $^{206}\text{Pb}/^{238}\text{U}$	\pm			
1.1	51	1	1.1	49.7	1.1	1.1	741	24	1.1	525	20	1.1	1718	27	1.1	48.5	1.3	1.1	1718	27	1.1	48.5	1.3
3.1	1853	29	2.1	51.8	1.1	1.2	734	17	2.1	1849	30	2.1	52.9	2.5	2.1	1.9	0.1	2.1	52.9	2.5	2.1	1.9	0.1
4.1	49	1	3.1	46.6	1.7	2.1	48.9	1.5	3.1	50.6	1.0	3.1	2674	91	3.1	9.3	0.5	3.1	2674	91	3.1	9.3	0.5
5.1	696	14	4.1	1544	39	4.1	65.0	1.6	4.1	52.2	0.9	4.1	1217	39	4.1	1795	39	4.1	1217	39	4.1	1795	39
6.1	49	2	5.1	1228	74	4.1	1559	68	5.1	1765	34	5.1	1.7	0.2	5.1	1441	21	5.1	1.7	0.2	5.1	1441	21
7.1	47	1	6.1	680	12	5.1	47.6	2.8	6.1	1622	114	6.1	1055	25	6.1	1821	39	6.1	1055	25	6.1	1821	39
8.1	48	1	7.1	49.0	1.1	6.1	47.9	1.4	7.1	8.9	0.6	7.1	34.1	1.9	7.1	1865	32	7.1	34.1	1.9	7.1	1865	32
9.1	1300	19	8.1	50.8	1.3	7.1	446	15	8.1	1049	23	8.1	2524	93	8.1	1888	58	8.1	2524	93	8.1	1888	58
10.1	1408	25	9.1	1861	91	8.1	837	23	9.1	1889	28	9.1	49.0	2.0	9.1	57.1	2.1	9.1	49.0	2.0	9.1	57.1	2.1
11.1	2105	24	10.1	545	19	9.1	47.5	1.5	10.1	1109	14	10.1	50.9	1.2	10.1	2030	30	10.1	50.9	1.2	10.1	2030	30
12.1	49	1	11.1	1751	28	10.1	85.6	3.9	11.1	1249	46	11.1	6.3	0.4	11.1	1119	31	11.1	6.3	0.4	11.1	1119	31
13.1	696	14	12.1	48.9	1.5	11.1	49.1	2.8	12.1	50.4	0.8	12.1	1181	30	12.1	1644	59	12.1	1181	30	12.1	1644	59
14.1	1505	27	13.1	47.9	2.6	12.1	1135	101	13.1	1285	14	13.1	1342	35	13.1	1630	26	13.1	1342	35	13.1	1630	26
15.1	48	1	14.1	48.2	2.3	13.1	80.3	2.8	14.1	1227	18	14.1	1542	37	14.1	1679	32	14.1	1542	37	14.1	1679	32
16.1	655	18	15.1	48.2	2.7	14.1	1747	48	15.1	1279	15	15.1	32.1	2.0	15.1	1638	35	15.1	32.1	2.0	15.1	1638	35
17.1	49	1	16.1	47.8	1.5	15.1	47.0	1.9	16.1	49.3	1.1	16.1	1590	32	16.1	48.2	1.5	16.1	1590	32	16.1	48.2	1.5
18.1	49	1	17.1	573	21	16.1	45.4	2.4	17.1	525	24	17.1	452	7	17.1	1597	37	17.1	452	7	17.1	1597	37
19.1	2445	54	18.1	1836	51	17.1	44.8	1.6	18.1	1204	15	18.1	2700	84	18.1	1651	33	18.1	2700	84	18.1	1651	33
20.1	691	9	19.1	50.2	2.2	18.1	48.1	1.5	19.1	506	8	19.1	1633	76	19.1	1665	39	19.1	1633	76	19.1	1665	39
21.1	49	1	20.1	49.3	1.2	19.1	46.9	1.7	20.1	47.7	1.3	20.1	7.1	0.3	20.1	2624	59	20.1	7.1	0.3	20.1	2624	59
22.1	47	1	21.1	2407	68	20.1	27.4	0.9	21.1	49.8	1.3	21.1	49.5	1.2	21.1	51.1	1.8	21.1	49.5	1.2	21.1	51.1	1.8
23.1	48	1	22.1	1614	47	21.1	338	13	22.1	149	8	22.1	1693	24	22.1	1740	21	22.1	1693	24	22.1	1740	21
24.1	2062	28	23.1	49.1	3.7	22.1	48.0	1.3	23.1	1523	28	23.1	1.9	0.4	23.1	1.6	0.7	23.1	1.9	0.4	23.1	1.6	0.7
25.1	46	2	24.1	50.5	2.1	23.1	620	14	24.1	509	11	24.1	5.9	0.4	24.1	1915	28	24.1	5.9	0.4	24.1	1915	28
26.1	107	5	25.1	48.5	2.9	24.1	680	18	25.1	963	14	25.1	1949	24	25.1	648	7	25.1	1949	24	25.1	648	7
27.1	1392	16	26.1	648	21	25.1	757	32	26.1	50.0	0.8	26.1	1379	15	26.1	1418	16	26.1	1379	15	26.1	1418	16
28.1	207	4	27.1	729	14	26.1	1717	36	27.1	1773	30	27.1	1666	31	27.1	48.7	0.7	27.1	1666	31	27.1	48.7	0.7
29.1	1479	23	28.1	46.3	4.5	27.1	82.1	3.5	28.1	1578	25	28.1	2664	61	28.1	1035	27	28.1	2664	61	28.1	1035	27
30.1	1492	28	29.1	45.6	3.0	28.1	45.6	1.8	29.1	1890	31	29.1	1727	18	29.1	2536	35	29.1	1727	18	29.1	2536	35
31.1	1707	23	30.1	48.9	1.9	29.1	47.8	1.4	30.1	1750	14	30.1	1466	30	30.1	1351	20	30.1	1466	30	30.1	1351	20
32.1	50.5	0.8	31.1	48.9	1.9	30.1	46.5	1.2	31.1	1538	41	31.1	47.9	1.0	31.1	1925	30	31.1	47.9	1.0	31.1	1925	30
33.1	48.8	1.2	32.1	1753	48	31.1	48.1	1.4	32.1	1508	27	32.1	77.2	1.4	32.1	48.2	1.0	32.1	77.2	1.4	32.1	48.2	1.0
34.1	710	42	33.1	44.1	2.6	32.1	653	15	33.1	496	11	33.1	1865	33	33.1	49.9	1.2	33.1	1865	33	33.1	49.9	1.2
35.1	1505	23	34.1	51.2	2.7	33.1	1006	42	34.1	1159	31	34.1	676	9	34.1	47.8	0.7	34.1	676	9	34.1	47.8	0.7
36.1	1804	27	35.1	91.2	7.2	34.1	50.9	1.8	35.1	1838	30	35.1	2344	57	35.1	50.4	0.9	35.1	2344	57	35.1	50.4	0.9
37.1	48.5	1.6	36.1	41.8	1.9	35.1	42.5	1.6	36.1	896	32	36.1	48.6	0.8	36.1	48.6	2.3	36.1	48.6	0.8	36.1	48.6	2.3
38.1	696	11	37.1	679	22	36.1	1817	156	37.1	10.4	0.7	37.1	1981	23	37.1	1785	51	37.1	1981	23	37.1	1785	51
39.1	49.6	0.7	38.1	45.3	1.1	37.1	47.1	1.2	38.1	534	12	38.1	1531	15	38.1	1548	46	38.1	1531	15	38.1	1548	46
40.1	1030	18	39.1	595	14	38.1	47.1	1.5	39.1	1617	27	39.1	1405	16	39.1	1544	38	39.1	1405	16	39.1	1544	38
41.1	48.4	1.0	40.1	46.5	1.0	39.1	37.2	1.3	40.1	858	35	40.1	36.0	0.5	40.1	1756	52	40.1	36.0	0.5	40.1	1756	52
42.1	1764	26	41.1	43.3	1.5	40.1	45.4	1.4	41.1	47.9	1.1	41.1	1526	27	41.1	1699	24	41.1	1526	27	41.1	1699	24
43.1	46.1	1.0	42.1	43.3	1.5	41.1	48.1	2.9	42.1	475	12	42.1	2827	58	42.1	1210	30	42.1	2827	58	42.1	1210	30
44.1	48.8	1.5	43.1	1511	51	42.1	1855	44	43.1	3359	229	43.1	1780	26	43.1	1721	100	43.1	1780	26	43.1	1721	100
45.1	2890	54	44.1	89.9	1.7	43.1	57.9	1.5	44.1	1019	16	44.1	43.2	2.5	44.1	983	13	44.1	43.2	2.5	44.1	983	13
46.1	46.9	0.8	45.1	48.4	2.3	44.1	46.9	2.3	45.1	48.6	0.9	45.1	1260	21	45.1	1840	22	45.1	1260	21	45.1	1840	22
47.1	1631	37	46.1	1296	37	45.1	138	10	46.1	50.8	2.3	46.1	1327	22	46.1	1398	32	46.1	1327	22	46.1	1398	32
48.1	2231	40	47.1	645	32	46.1	46.5	3.1	47.1	1839	27	47.1	1473	26	47.1	49.6	0.8	47.1	1473	26	47.1	49.6	0.8
49.1	49.5	0.9	48.1	49.3	2.4	47.1	49.7	3.7	48.1	1223	30	48.1	757	10	48.1	1860	35	48.1	757	10	48.1	1860	35
50.1	49.1	1.2	49.1	1348	27	48.1	49.7	3.7	49.1	112	7	49.1	50.1	7	49.1	50.1	7	49.1	50.1	7	49.1	50.1	7

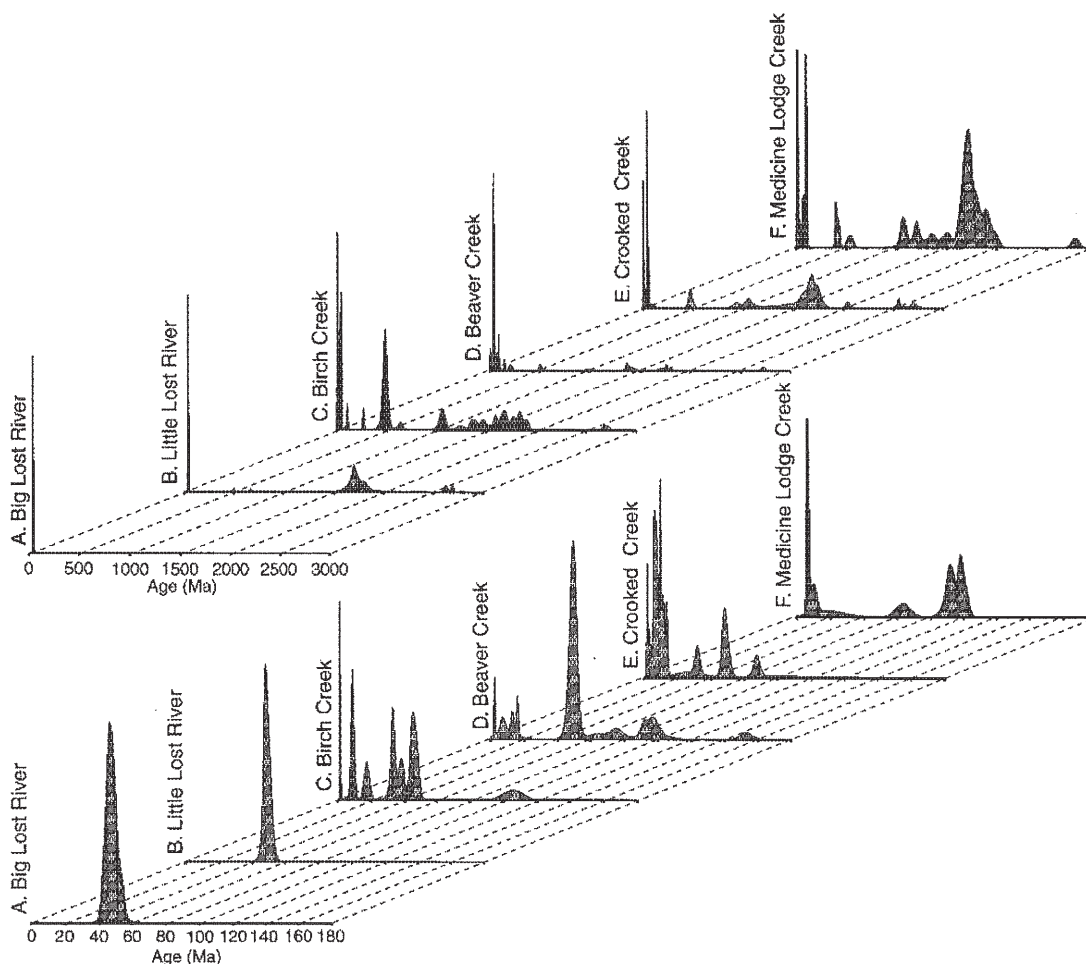


Figure 4. Relative probability plots for detrital-zircon ages determined for modern fluvial sands. Big Lost River, Little Lost River, and Birch Creek (A–C) are primary fluvial systems flowing into Big Lost Trough; smaller streams (D–F) are north of basin. Upper graphs contain results of all analyses (0–3000 Ma zircons); lower graphs are for young (<180 Ma) zircon populations.

River sample (Fig. 4A) is characterized by an abundance of ca. 50 Ma zircon grains and by a relative lack of older zircons.

Subsurface sands from well 2-2A in the central Big Lost Trough have detrital-zircon age spectra (Fig. 5) that are characterized by an abundance of ca. 50 Ma zircons and very few Paleozoic and older zircon grains. Small populations of 70–100 Ma zircons probably indicate derivation from the Cretaceous Idaho batholith. On the basis of visual comparison, detrital-zircon age spectra for these samples are most similar to the age spectra for the modern Big Lost River (Fig. 4A). These data suggest that the Big Lost River drainage was the dominant source, and are in agreement with modal compositional data (Fig. 3).

Subsurface samples from core collected in wells at TAN, near the northern margin of the basin, have detrital-zircon age spectra (Fig. 6) that suggest changing source areas through time. The detrital-zircon age spectrum of a near-surface sand

sample (depth of 6.1–7.6 m in TAN-34; Fig. 6A) is most similar to the signature of the Big Lost River (Fig. 4A). However, deeper samples (Fig. 6, B–D) have detrital-zircon signatures similar to Birch Creek (Fig. 4C) or Crooked Creek (Fig. 4E).

Mineralogy of fine-grained sediments

The compositions of fine-grained sediments from surficial lacustrine and playa deposits were evaluated and compared to fine-grained deposits from the shallow subsurface (Figs. 7 and 8). X-ray diffraction analysis was used to determine the semi-quantitative mineralogy of the <4 μm fraction of the samples, typically clay and evaporite minerals. Semi-quantitative mineral abundance was based on the relative intensity of the diffraction peak for the clay or evaporite mineral. Material comprising the remainder of the samples, including quartz silt to very fine sand, organic matter, and detrital or authigenic carbonate, was not

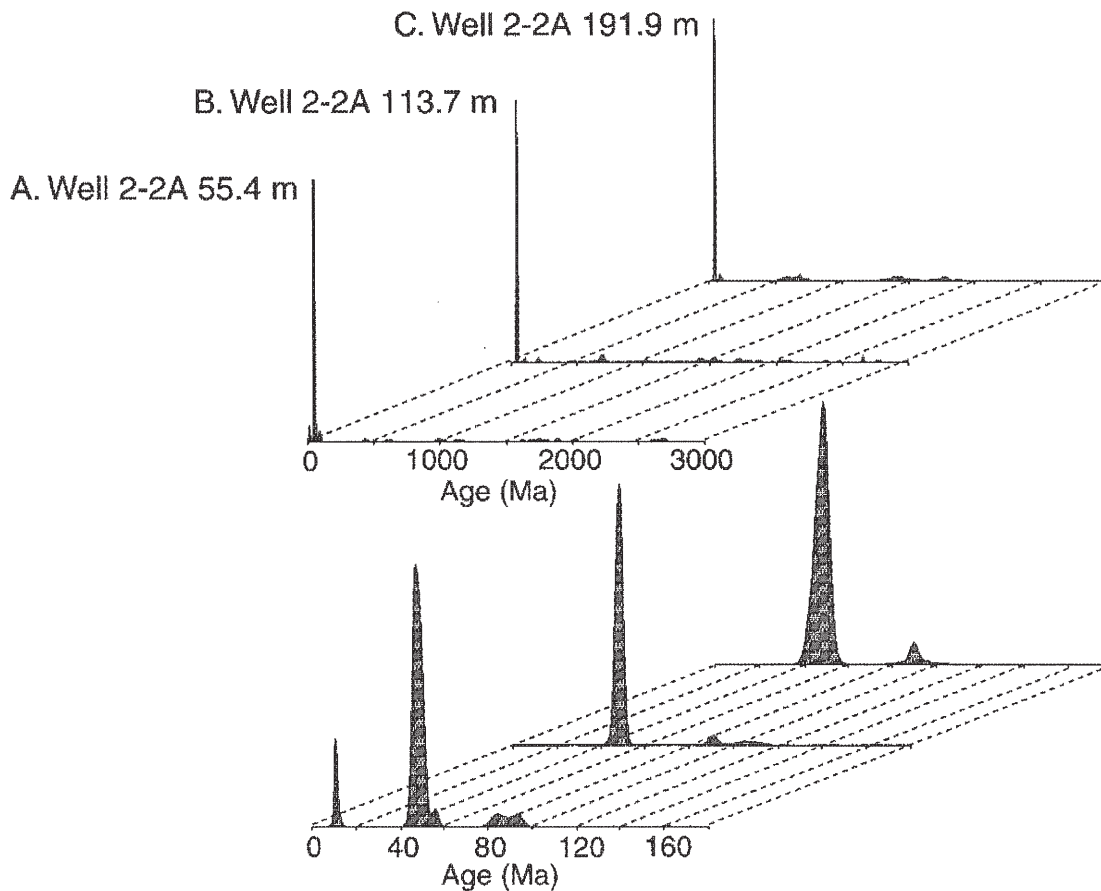


Figure 5. Relative probability plots for detrital-zircon ages determined for subsurface sands from well 2-2A, in middle of Big Lost Trough (Fig. 1). Upper graphs contain results of all analyses (0–3000 Ma zircons); lower graphs are for young (<180 Ma) zircon populations.

analyzed. Analysis of the samples included glycolization, to determine the presence of expanding clays (e.g., smectite), and 550°C heat treatment to differentiate chlorite and kaolinite.

X-ray diffraction data for shallow subsurface samples from well 2-2A (Fig. 8A) are generally similar to the surficial lacustrine and playa deposits (Fig. 7) in that they contain primarily smectite, kaolinite, and chlorite. This mineral assemblage probably reflects weathering of abundant volcanic and sedimentary rocks in fluvial source areas. However, several samples from the TAN wells (Fig. 8B) are distinctly different in that they contain gypsum. These data suggest that ancient evaporative playas or evaporative marginal lacustrine environments existed along the margin of the basin and that climatic conditions during deposition were probably drier than modern conditions.

DISCUSSION

The geometry and stratigraphic architecture of the Big Lost Trough was strongly influenced by the volcanic rift zones that define most of the basin margins. The locations of these vol-

canic rift zones, as well as local and regional subsidence patterns, reflect the interaction between basaltic volcanism and rhyolite caldera formation related to the Yellowstone hotspot and development of Basin and Range structures. Offlapping basalt flow groups and onlapping clastic sedimentary units along the northern margin of the basin (e.g., Fig. 2) represent growth of the volcanic rift zones and simultaneous clastic sedimentation in the basin. A general volcanic quiescence over the past ~1 m.y. has allowed fluvial, playa, eolian, and lacustrine systems to infill the basin to its modern configuration (Fig. 2C).

Sediments deposited in the middle of the basin over the past ~1 m.y. contain fluvial, eolian, and minor playa deposits interbedded with lacustrine sediment; this could represent alternating relatively wetter and relatively drier climatic conditions. This argument is based on documented fluctuations of Lake Terretton over the past 2 m.y. (e.g., Scott, 1982; Gianniny et al., this volume) and the presence of fluvial sands from the Big Lost River in the middle of the basin (Figs. 3–6).

Provenance studies in the Big Lost Trough that involve a comparison of modern fluvial and eolian sands with sands from

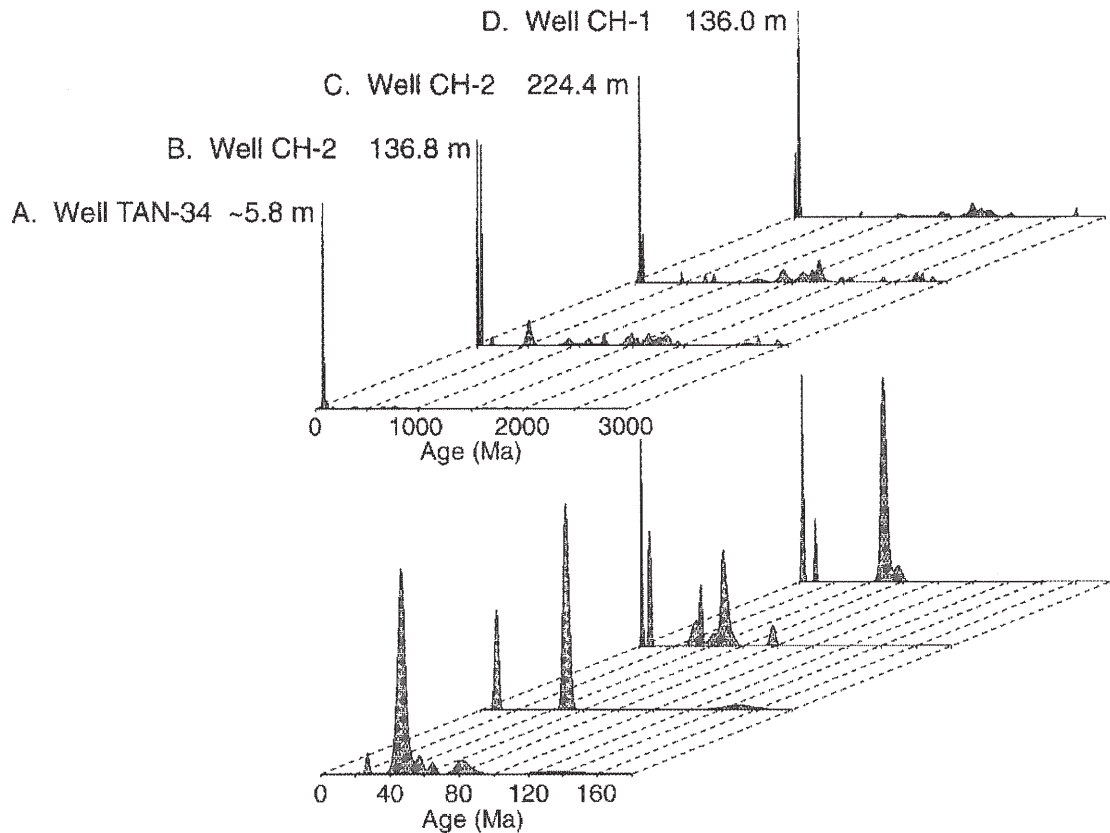


Figure 6. Relative probability plots for detrital-zircon ages determined for subsurface sands from wells at Test Area North, along northeastern margin of Big Lost Trough (Fig. 1). Upper graphs contain results of all analyses (0–3000 Ma zircons); lower graphs are for young (<180 Ma) zircon populations.

the subsurface using both petrography and U/Pb geochronology of detrital zircons provide very robust correlations (Figs. 4–6; Geslin et al., 1999). However, relating the detrital-zircon age spectra from modern Big Lost River sand and correlative subsurface sands to those of bedrock exposures in the source area is somewhat difficult. It is surprising that the Proterozoic to Archean detrital-zircon signature in these samples is faint despite the fact that the upper reaches of the Big Lost River drain the Pioneer Mountains core complex (Fig. 1), where abundant Paleoproterozoic metamorphic rocks crop out (Worl et al., 1995). Possible explanations for this observation include: (1) the great abundance of Eocene Challis volcanics cropping out in the middle reaches of the river have diluted the detrital zircon population; or (2) smaller streams that drain the Pioneer Mountains core complex were captured by the Big Lost River relatively recently, and Proterozoic to Archean zircons have yet to be transported to the lower reaches of the river. These data suggest that provenance determination, even in a well-documented setting like the Big Lost Trough, is a complex task, and that the zircon signature of the Big Lost River requires further study (e.g., Link et al., 1999, 2000).

Subsurface sands in the middle of the Big Lost Trough have provenance signatures indicating deposition by the Big

Lost River, suggesting that the proportion of Big Lost River fluvial sand in the subsurface increases from northeast to southwest, toward the point where the river enters the basin (Fig. 1). The southwestward increase in abundance of subsurface sand-rich sediments, the increase in the thickness of strata from the northern basin margin to basin center (Fig. 2C), and the regional northeast to southwest groundwater gradient all suggest that water flowing in the upper part of the Snake River Plain aquifer will encounter progressively more abundant and more conductive sediments as it migrates down gradient from the TAN facilities toward the middle of the basin. This information should be incorporated into regional hydrologic models of the unsaturated zone and upper part of the Snake River Plain aquifer.

CONCLUSIONS

The Big Lost Trough is an arid underfilled basin, the geometry and volcanic-sedimentary stratigraphic architecture of which reflect the development of surrounding volcanic rift zones. The pattern of volcanic rift zones that define the basin margins, subsidence of the area, and the fluvial systems that provide clastic sediments to the basin reflect the interaction of the migrating Yellowstone hotspot and developing Basin and

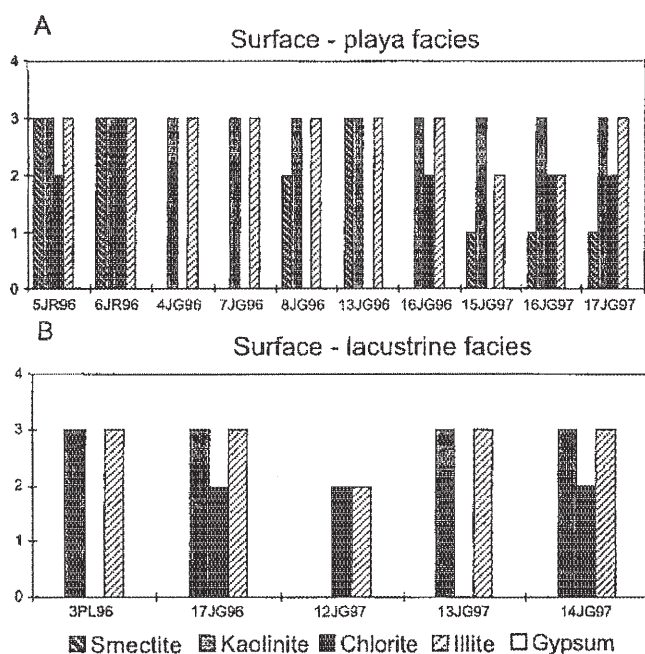


Figure 7. Semiquantitative mineralogy of fine-grained fraction of surficial playa and lacustrine sediments determined using X-ray diffraction analyses. Ranking from 0 to 4 indicates relative abundance of mineral: 4 = mineral dominant in sample, 3 = mineral present in sample, 2 = trace amounts of mineral in sample, 1 = mineral possibly present in sample.

Range structures. Correlations of basalt flow groups and sedimentary successions from the basin margin at TAN to the middle of the basin at well 2-2A show the complex stratigraphic relationships created by basalt flows that downlap into the basin and sediments that onlap onto the adjacent volcanic high. Architecture within the clastic sedimentary fill of the basin reflects deposition during climatically influenced progradation and retrogradation of a fluvial-playa-eolian depositional system and transgressions and regressions of Lake Terreton.

Because the Big Lost Trough is still an active basin with easily identifiable sediment source areas, it provides an excellent natural laboratory for conducting provenance studies. By conducting both petrographic and U/Pb detrital-zircon geochronology analyses on subsurface sands, as well as modern fluvial and eolian deposits, the provenance of the subsurface sands has been very tightly defined. These analyses suggest that the Big Lost River has been the dominant source of sediment to the basin for at least the past 1 m.y., and that the river system frequently prograded across the basin during lowstands of Lake Terreton. Fluvial progradation during lowstands of Lake Terreton was associated with eolian reworking of fluvial deposits.

Semiquantitative compositional analyses, using X-ray diffraction, indicate that subsurface playa or marginal lacustrine deposits along the basin margin (at TAN) contain abundant gypsum, suggesting that ancient dry climate cycles were drier than the modern dry climate.

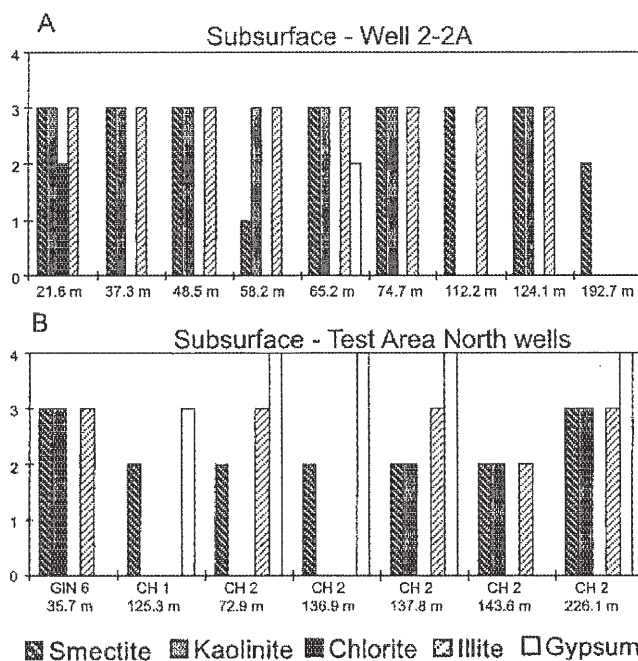


Figure 8. Semiquantitative mineralogy of fine-grained fraction of subsurface deposits determined using X-ray diffraction analyses for samples from well 2-2A, in middle of basin, and from wells at Test Area North, along northeastern margin of basin. Ranking from 0 to 4 indicates relative abundance of mineral: 4 = mineral dominant in sample, 3 = mineral present in sample, 2 = trace amounts of mineral in sample, 1 = mineral possibly present in sample.

ACKNOWLEDGMENTS

This study was funded by grant DE-FG07-96ID13420 from the Department of Energy to the Idaho Water Resources Research Institute and Idaho Universities Consortium. Mary Kauffman and Savona Anderson assisted with sample collection and analysis. Fruitful discussions of sedimentary systems on the Snake River Plain were held with Gary Gianniny and Glenn Thackray. Access to core was provided by Linda Davis (U.S. Geological Survey). The manuscript was improved by comments from reviewers Larry Middleton, Dick Smith, and Brad Ritts.

REFERENCES CITED

- Anders, M.H., Geissman, J.W., Piety, L., and Sullivan, T., 1989, Parabolic distribution of circum-eastern Snake River Plain seismicity and latest Quaternary faulting: mMigratory pattern and association with the Yellowstone hotspot: *Journal of Geophysical Research*, v. 94, p. 1589-1621.
- Anderson, S.R., 1991, Stratigraphy of the unsaturated zone and uppermost part of the Snake River Plain aquifer at the Idaho Chemical Processing Plant and Test Reactors Area, Idaho National Engineering Laboratory, Idaho: U.S. Geological Survey Water-Resources Investigations Report 91-4010, 71 p.
- Anderson, S.R., and Bowers, B., 1995, Stratigraphy of the unsaturated zone and uppermost part of the Snake River Plain aquifer at Test Area North, Idaho National Engineering Laboratory, Idaho: U.S. Geological Survey Water-Resources Investigations Report 95-4130, 47 p.

- Anderson, S.R., and Lewis, B.D., 1989, Stratigraphy of the unsaturated zone at Radioactive Waste Management Complex, Idaho National Engineering Laboratory, Idaho: U.S. Geological Survey Water-Resources Investigations Report 89-4065, 54 p.
- Anderson, S.R., Liszewski, M.J., and Ackerman, D.J., 1996, Thickness of surficial sediment at and near the Idaho National Engineering Laboratory, Idaho: U.S. Geological Survey Open-File Report 96-330, 16 p.
- Blair, J.J., and Link, P.K., 2000, Pliocene and Quaternary sedimentation and stratigraphy of the Big Lost Trough from coreholes at the Idaho National Engineering and Environmental Laboratory, Idaho: Evidence for a regional Pliocene lake during the Olduvai normal polarity subchron. *in* Robinson, L., ed., Proceedings of the 35th Symposium on Engineering Geology and Geotechnical Engineering: Pocatello, Idaho, Idaho State University, College of Engineering, p. 163-179.
- Carroll, A.R., and Bohacs, K.M., 1999, Stratigraphic classification of ancient lakes: Balancing tectonic and climatic controls: *Geology*, v. 27, p. 99-102.
- Champion, D.E., Lanphere, M.A., and Kuntz, M.A., 1988, Evidence for a new geomagnetic reversal from lava flows in Idaho: Discussion of short polarity reversals in the Brunhes and late Matuyama polarity chrons: *Journal of Geophysical Research*, v. 93, p. 11667-11680.
- Evans, K.V., and Zartman, R.E., 1988, Early Paleozoic alkalic plutonism in east-central Idaho: *Geological Society of America Bulletin*, v. 100, p. 1981-1987.
- Geslin, J.K., Gianniny, G.L., Link, P.K., and Riesterer, J.W., 1997, Subsurface sedimentary facies and Pleistocene stratigraphy of the northern Idaho National Engineering Laboratory: Controls on hydrogeology, *in* Sharma, S., and Hardcastle, J. H., eds., Proceedings of the 32nd Annual Symposium on Engineering Geology and Geotechnical Engineering: Moscow, Idaho, University of Idaho, p. 15-28.
- Geslin, J.K., Link, P.K., and Fanning, C.M., 1999, High-precision provenance determination using detrital-zircon ages and petrography of Quaternary sands on the eastern Snake River Plain, Idaho: *Geology*, v. 27, p. 295-298.
- Gianniny, G.L., Geslin, J.K., Riesterer, J.W., Link, P.K., and Thackray, G.D., 1997, Quaternary surficial sediments near Test Area North (TAN), north-eastern Snake River Plain: An actualistic guide to aquifer characterization, *in* Sharma, S., and Hardcastle, J.H., eds., Proceedings of the 32nd Annual Symposium on Engineering Geology and Geotechnical Engineering: Moscow, Idaho, University of Idaho, p. 29-44.
- Hackett, W.R., and Smith, R.P., 1992, Quaternary volcanism, tectonics, and sedimentation in the Idaho National Engineering Laboratory area: *in* Wilson J.R., ed., Field guide to geologic excursions in Utah and adjacent areas of Nevada, Idaho, and Wyoming: Utah Geological Survey Miscellaneous Publication 92-3, p. 1-18.
- Ingersoll, R.V., Bullard, R.R., Ford, R.L., Grimm, J.P., Pickel, J.P., and Sares, S.W., 1984, The effect of grain size on detrital modes: A test of the Gazzi-Dickinson point-counting method: *Journal of Sedimentary Petrology*, v. 54, p. 103-116.
- Kuntz, M.A., Covington, H.R., and Schorr, L.J., 1992, An overview of basaltic volcanism of the eastern Snake River Plain, Idaho, *in* Link, P.K., Kuntz, M.A., and Platt, L.B., eds., Regional geology of eastern Idaho and western Wyoming: Geological Society of America Memoir 179, p. 227-267.
- Kuntz, M.A., Skipp, B., Lanphere, M.A., Scott, W.E., Pierce, K.L., Dalrymple, G.B., Champion, D.E., Embree, G.F., Page, W.R., Morgan, L.A., Smith, R.P., Hackett, W.R., and Rodgers, D.W., 1994, Geological map of the Idaho National Engineering Laboratory and adjoining areas, eastern Idaho: U.S. Geological Survey Miscellaneous Investigations Series Map I-2330, scale 1:100 000.
- Lanphere, M.A., Kuntz, M.A., and Champion, D.E., 1994, Petrography, age, and paleomagnetism of basaltic lava flows in coreholes at the Test Area North (TAN), Idaho National Engineering Laboratory: U.S. Geological Survey Open-File Report 94-686, 49 p.
- Link, P.K., Geslin, J.K., Thackray, G.T., Gianniny, G.L., 1999, Basin architecture of the Pleistocene Bit Lost Trough, eastern Snake River Plain, Idaho: Geological Society of America Abstracts with Programs, v. 31, no. 4, p. A22.
- Link, P.K., Geslin, J.K., and Fanning, C.M., 2000, Detrital zircon 'barcodes' from modern and Neogene sands of the Snake River Plain, Idaho: Defining a provenance area requires several grains and single grains mean little: Geological Society of America Abstracts with Programs, v. 32, no. 6, p. A25.
- Morgan, L. A., 1992, Stratigraphic relations and paleomagnetic and geochemical correlations of ignimbrites of the Heise Volcanic Field, Eastern Snake River Plain, eastern Idaho and western Wyoming, *in* Link, P.K., Kuntz, M.A., and Platt, L.B., eds., Regional geology of eastern Idaho and western Wyoming, Geological Society of America Memoir 179, p. 215-226.
- Morgan, L.A., Doherty, D.J., and Leeman, W.P., 1984, Ignimbrites of the eastern Snake River Plain: Evidence for major caldera forming eruptions: *Journal of Geophysical Research*, v. 89, p. 8665-8678.
- McQuarrie, N., and Rodgers, D.W., 1998, Subsidence of a volcanic basin by flexure and lower crustal flow: The eastern Snake River Plain, Idaho: *Tectonics*, v. 17, p. 203-220.
- Nace, R.L., Voegeli, P.T., Jones, J.R., and Deutsch, M., 1975, Generalized geologic framework of the National Reactor Testing Station, Idaho: U.S. Geological Survey Professional Paper 725-B, 49 p.
- Oaks, R.Q., Jr., James, W.C., Francis, G.G., and Schulingkamp, W.J., 1977, Summary of Middle Ordovician stratigraphy and tectonics, northern Utah, southern and central Idaho, *in* Heisey, E.L., Lawson, D.E., Norwood, E.R., Wach, P.H., and Hale, L.A., eds., Rocky Mountain thrust belt geology and resources: Casper, Wyoming, Wyoming Geological Association Guidebook, p. 101-118.
- Pierce, K.L., and Morgan, L.A., 1992, The track of the Yellowstone hot spot, *in* Link, P.K., Kuntz, M.A., and Platt, L.B., eds., Regional geology of eastern Idaho and western Wyoming: Geological Society of America Memoir 179, p. 1-53.
- Scott, W.E., 1982, Surficial geologic map of the eastern Snake River Plain and adjacent areas, 111°-115° W, Idaho and Wyoming: U.S. Geological Survey Miscellaneous Investigations Series Map I-1372, scale 1:250000, 2 sheets.
- Skipp, B., and Link, P.K., 1992, Middle and Late Proterozoic rocks and Late Proterozoic tectonics in the southern Beaverhead Mountains, Idaho and Montana, a preliminary report, *in* Link, P.K., Kuntz, M.A., and Platt, L.B., eds., Regional geology of eastern Idaho and western Wyoming: Geological Society of America Memoir 179, p. 141-153.
- Spinazoła, J.M., 1994, Geohydrology and simulation of flow and water levels in the aquifer system in the Mud Lake area of the eastern Snake River Plain, eastern Idaho: U.S. Geological Survey Water-Resources Investigations Report 93-4227, 78 p.
- Stearns, H.T., Crandall, L., and Steward, W.G., 1939, Geology and groundwater resources of the Mud Lake region, Idaho, including the Island Park area: U.S. Geological Survey Water-Supply Paper 818, 125 p.
- Whitehead, R.L., 1992, Geohydrologic framework of the Snake River Plain regional aquifer system, Idaho and eastern Oregon: U.S. Geological Survey Professional Paper 1409-B, 32 p., 6 plates.
- Winston, D., and Link, P.K., 1993, Middle Proterozoic rocks of Montana, Idaho, and Washington: The Belt Supergroup, *in* Reed, J., Simms, P., Houston, R., Rankin, D., Link, P., Van Schmus, R., and Bickford, P., eds., Precambrian of the conterminous United States: Boulder, Colorado, Geological Society of America, *Geology of North America*, v. C-3, p. 487-521.
- Worl, R.G., Link, P.K., Winkler, G.R., and Johnson, K.M., editors., 1995, Geology and mineral resources of the Hailey 1° × 2° quadrangle and the western part of the Idaho Falls 1° × 2° quadrangle, Idaho: Washington, D.C., U.S. Geological Survey Bulletin 2064, v. 1, chapters A-R, separate pagination.